

Published in final edited form as:

*J Am Chem Soc.* 2013 July 31; 135(30): 10906–10909. doi:10.1021/ja4042687.

## Deconstructing activation events in rhodopsin

 Elena N. Laricheva<sup>†</sup>, Karunesh Arora<sup>†</sup>, Jennifer L. Knight<sup>†</sup>, and Charles L. Brooks III<sup>\*,†,‡</sup>
<sup>†</sup>Department of Chemistry, University of Michigan, Ann Arbor, Michigan 48109, United States

<sup>‡</sup>Biophysics Program, University of Michigan, Ann Arbor, Michigan 48109, United States

### Abstract

Activation of class A G-protein coupled receptors (GPCRs) involves large-scale reorganization of the H3/H6 interhelical network. In rhodopsin (Rh), this process is coupled to a change in the protonation state of a key residue, E134, whose exact role in activation is not well understood. Capturing this millisecond pH-dependent process is a well-appreciated challenge. We developed a scheme combining the Harmonic Fourier Beads (HFB) method and constant pH molecular dynamics with pH-based replica exchange (pH-REX) to gain insight into the structural changes occurring along the activation pathway as a function of change in the protonation state of E134. Our results indicate that E134 protonates as a consequence of H6 tilting by *ca.* 4.0° with respect to its initial position and simultaneously rotating by *ca.* 23° along its principal axis. The movement of H6 is associated with the breakage of the E247-R135 and R135-E134 salt bridges and concomitant release of the E134 side chain, which results in the increase of its pK<sub>a</sub> value above physiological pH. An increase in the hydrophobicity of the environment surrounding E134 leads to further tilt and rotation of H6 and upshift of the E134 pK<sub>a</sub>. Such atomic-level information, otherwise not accessible to experiments, refines the earlier proposed sequential model of Rh activation (Zaitseva, E.; et al. Sequential Rearrangement of Interhelical Networks Upon Rhodopsin Activation in Membranes: The Meta II<sub>a</sub> Conformational Substate. *J. Am. Chem. Soc.* **2010**, *132*, 4815) and argues that the E134 protonation switch is both a cause and a consequence of the H6 motion.

A hallmark of the transition between inactive and active forms of heptahelical G-protein coupled receptors (GPCRs) is the large (3–14 Å) outward tilt of transmembrane helix 6 (H6) in response to various extracellular stimuli, such as light or ligand binding.<sup>1,2</sup> This tilt causes rearrangements in the H3/H6 interhelical network and creates a cavity for the binding of the heterotrimeric G-protein, thus initiating a cascade of signaling events inside a cell.<sup>3</sup> In rhodopsin (Rh), the most widely studied member of class A GPCRs, there are several pre- and post-requisites for the H6 motion, including a series of conformational and protonation switches at the late stages of activation.<sup>4,5</sup> Following ultrafast 11-*cis* to all-*trans* photoisomerization<sup>6</sup> of the retinal protonated Schiff base (11-PSB), formed by the chromophore retinal covalently bound to K296, the signal is propagated from the dark state through a series of inactive intermediates to a cytoplasmic receptor domain where a signaling Meta II state capable of binding the G-protein is formed (Figure 1A).<sup>3,7</sup>

While early transitions can be exclusively described by the small-scale rearrangements in the retinal binding pocket adjusting to accommodate the isomerized chromophore,<sup>8</sup> the major functional and structural changes of the  $\alpha$ -helical bundle occur during the pH-

\*Corresponding Author brookscl@umich.edu.

Supporting Information. Details of the computational protocol and analysis. This material is available free of charge via the Internet at <http://pubs.acs.org>.

The authors declare no competing financial interests.

dependent Meta I to Meta II transition.<sup>9,10</sup> According to the activation scheme, originally proposed by Hofmann and Hubbell and colleagues<sup>11,12</sup> and later corroborated and extended by Vogel and co-workers,<sup>13,14</sup> this transformation occurs sequentially via a series of metastable states Meta II<sub>a</sub>, Meta II<sub>b</sub>, and Meta II<sub>b</sub>-H<sup>+</sup>, with the latter two collectively representing the Meta II form. Based on this scheme, Meta II<sub>a</sub> is formed upon disruption of the salt bridge between the all-trans protonated Schiff base (AT-PSB) and the primary counterion E113 via an internal proton transfer between the two moieties with the formation of an unprotonated Schiff base (AT-SB; first protonation switch; Figure 1B); Meta II<sub>b</sub> stems from the 6 Å outward tilt of H6; and Meta II<sub>b</sub>-H<sup>+</sup> is a result of the proton uptake by E134 of the conserved E(D)RY motif located on H3 near the cytoplasmic water/lipid interface (second protonation switch; Figure 1C). The suggested reaction scheme is supported by a number of experimental studies,<sup>9,11,12,14</sup> however a precise dynamic picture of how the proposed structural changes occur is still missing. Molecular dynamics (MD) simulations can provide a detailed answer to this question and, thus, have been widely exploited by different research groups.<sup>15</sup> However, capturing this millisecond transition is beyond the reach of standard MD simulations. Several attempts have been made to overcome the timescale limitation and to arrive at the Meta II state by running long MD guided by the NMR distance restraints starting from either the dark state<sup>16</sup> or, most recently, from lumirhodopsin.<sup>17</sup> These calculations, however, all assumed fixed protonation states during the dynamics and did not consider on-the-fly coupling between pH and conformational switching, as we do in the current work. Here, we delineate a sequence of late activation events in Rh by probing a conformational transition between its putative semi-active Meta II<sub>a</sub> and active Meta II forms as a function of change in the protonation state of E134.

We used the 4.15 Å (PDB entry 2I37) and the 3.0 Å (3PXO) X-ray structures to construct initial models of the Meta II<sub>a</sub> and Meta II states, respectively. We utilized the Generalized Born with a Simple Switching (GBSW)<sup>18,19</sup> implicit solvent/implicit membrane model to determine an optimal position of each structure in the membrane and used the corresponding lowest energy configurations as the starting points to generate a transition pathway between the initial Meta II<sub>a</sub> and final Meta II state using the Harmonic Fourier Beads method (HFB).<sup>20</sup> Prior to the pathway generation, constant pH molecular dynamics<sup>21</sup> with pH-based replica exchange (pH-REX)<sup>22</sup> was used to determine the protonation states of E113, E181, and E134 in the starting Meta II<sub>a</sub> and final Meta II states. E113 and E181 were found to be protonated in both states, so these residues were modeled as neutral in all subsequent simulations. Once the path was generated, pH-REX was used to capture the protonation of E134 along the conformational transition pathway. All calculations were performed using the CMAP-corrected<sup>23</sup> all-atom CHARMM22 force field for proteins<sup>24</sup>. For details of the computational methods and analysis see the Supporting Information.

Our results show that the pK<sub>a</sub> of E134 changes from 5.6 to 8.3 upon transition with a protonation switch (pK<sub>a</sub>=7.4) occurring early along the computed path (Figure 2A). This process is associated with the breakage of the E134–R135 and R135–E247 salt bridges, holding Rh in the semi-active conformation, and a subsequent formation of the new E247–K231 ionic lock stabilizing the Meta II state. The R135–E247 breaks first, releasing the side chain of E134 and allowing its pK<sub>a</sub> value to rise, as confirmed by the pK<sub>a</sub> switch at 7.4 shortly afterwards. The outward tilt of H6, monitored as the angle between the helical axis at each new point of the pathway relative to its initial position, is depicted in Figure 2B. The observed tilt is sequential (segments *a–b*, *b–c*, and *c–d*; green line) and is partially coupled to the rotation of H6 along its principal axis, which also occurs in a sequential manner (segments *a–b*, *b–c*, and *c–d*; red line). As shown, the E134 protonation switch, associated with breakage of the R135–E247 and E134–R135 salt bridges, is a consequence of H6 rotating by *ca.* 23° along the helical axis (segment *a–b*) and simultaneously tilting outwards by *ca.* 4°. Later (region *b–c*), the H6 tilt and rotation are partially decoupled with H6

continuing to tilt but not rotating anymore, while their coupled motion becomes apparent again along the *c-d* and *c'-d'* segments. The latter changes, characterized by an additional *ca.* 30° helical rotation and *ca.* 10° outward tilt, bringing the H5 and H6 extracellular ends together, accompanies the shift of the pK<sub>a</sub> of E134 from 7.4 to 8.3.

Our results are in apparent disagreement with the experimental interpretation suggesting that proton uptake by E134 in Rh does not happen unless H6 has fully moved.<sup>12-14</sup> These experimental conclusions are based on the observed pH independence of the EPR signal arising from the immobilization of the nitroxide side chain in the spin-labeled V227C Rh mutant (R227) in response to the outward tilt of H6.<sup>12</sup> In this mutant, R227 belongs to the neighboring helix H5 and senses the changes in the surrounding environment. Once the outward tilt of H6 in the direction of H5 becomes sufficiently large, the spin-label can sense the change in the environment and gives rise to the EPR signal. Since the maximum amplitude of the EPR signal remained the same in the entire pH range from 5 to 9, it was concluded that the E134 proton uptake followed H6 motion. Based on our results, we provide an alternative explanation of the observed pH independence of the EPR signal. Along segment *a-b*, an outward tilt of H6 is expected to be strongly pH as depicted in Figure S7. Thus, our results call for the re-interpretation of the EPR data on Rh and reconsideration of the existing activation scheme.

To understand the origin of the pK<sub>a</sub> shift, the solvent accessible surface area (SASA) of E134 was computed along the transition pathway (Figure 2C). It increases up to the point where the E134 protonation switch occurs, in agreement with the observed breakage of the E247-R135 and E134-R135 salt bridges releasing the side chain of E134 and exposing it to the solvent. Then, along the portion of the pathway corresponding to the shift of the pK<sub>a</sub> from 7.4 to 8.3, the SASA gradually drops indicating an increase in hydrophobicity of the environment surrounding the side chain of E134. As Figure 2D illustrates, this is in part due to a desolvation effect and displacement of the side chain from the water bulk dependent due to a large shift of the pK<sub>a</sub> of E134 (5.6 to 7.4), but the small tilt angle (*ca.* 4°) associated with it is insufficient to cause the immobilization of the spin label and a saturation of the EPR signal. The latter is confirmed by the small number of contacts that R227 makes with H6 along that portion of pathway (Figure S7). In contrast, along segment *b'-d*, associated with an easily detectable H6 tilt (*ca.* 10°), the pK<sub>a</sub> shift is significantly smaller (7.4 to 8.3) and the expected pH dependence of the tilt is small as well. Accordingly, the computed number of contacts along *b'-d* substantially increases, closer to the lipid/water interface, from L=-19.4 to L=-17.5, where L=-15 indicates a position of the lower membrane plane lying on the cytoplasmic side of the 30Å-thick implicit lipid bilayer used in our study.

Another important factor that contributes to the pK<sub>a</sub> shift is the exposure of the E134 side chain to the so-called “hydrophobic barrier,”<sup>25</sup> consisting of L76, L79, L128, L131, M253, M257. Structural rearrangements of the E(D)RY motif with respect to this region along the Meta II<sub>a</sub> to Meta II transition pathway are shown in Figure 2 (structures I, II and III). Upon breakage of the E247-R135 and E134-R135 salt bridges preceding the E134 protonation switch, the released E134 side chain makes close contacts with L128 and L131 and becomes deeply buried inside the protein. The more hydrophobic environment stabilizes the neutral form of E134 and leads to a shift of its pK<sub>a</sub> from 7.4 to 8.3. Notably, no experimental data exists for the pK<sub>a</sub> values of the ionizable residues in Rh, however, our predictions agree well with the change of the E134 protonation state determined experimentally,<sup>26,27</sup> as well as with the electrostatic MM-SCP calculations by Periole et al.<sup>28</sup> It is also worth noting that CPHMD calculations based on the GBSW implicit solvent model have been successfully applied to many proteins<sup>29-32</sup> where comparison between experimental and computed values could be rigorously made yielding the RMSE of 0.6 pH units for proteins containing few buried ionizable side chains.<sup>29</sup> Given the precision of the pK<sub>a</sub> values in our simulations,

the shift in  $pK_a$  from 7.4 to 8.3 that we observe is statistically significant at the 95% confidence interval and so the observed change reflects conformational dynamics of the protein and allows us to delineate a sequence of activation events using the protonation state of E134 as a reaction coordinate.

Overall, the results of our study combining the HFB method and pH-REX simulations enable us to derive a detailed mechanistic picture of the late activation events in Rh and elucidate mechanistic details of coupling between the change in the protonation state of E134 and conformational dynamics of the protein. The HFB made it possible to explore the reaction pathway without making any prior assumptions about the reaction mechanism, and the pH-REX performed at every point of the pathway allowed us to incorporate the information about the protonation state of E134 on-the-fly and, thus, probe an existing sequential Meta II<sub>a</sub>–Meta II<sub>b</sub>–Meta II<sub>b</sub>-H<sup>+</sup> reaction scheme.<sup>10–12</sup> While the experimental data suggests that proton uptake by Glu134 is a consequence of H6 motion, our simulations offer an alternative explanation. We show that E134 protonates early along the computed path as a consequence of H6 tilting by *ca.* 4.0° with respect to the membrane normal and simultaneously rotating by *ca.* 23° along the helical axis. This process is associated with the breakage of the E247-R135 and R135-E134 salt bridges releasing the side chain of E134 and allowing it to raise its  $pK_a$  value above physiological pH. This, in turn, leads to a further *ca.* 10° tilt and *ca.* 30° rotation of H6 together with the 2–3 Å translation of the E134 side chain towards the center of the membrane causing the upshift of its  $pK_a$ . In the first segment of the pathway, the expected pH dependence of the H6 tilt, associated with the significant difference in the  $pK_a$  of E134 (5.6 to 7.4), is large, but the small value of the tilt is, we argue, insufficient to cause an immobilization of the spin label in the EPR experiment and saturate the EPR signal. In the second region, however, the tilt is large enough to be observed, but the expected pH dependence of the tilt is negligible owing to a two-fold smaller modulation of the  $pK_a$  shift.

## Supplementary Material

Refer to Web version on PubMed Central for supplementary material.

## Acknowledgments

This work was supported by the NIH (GM037554 and GM057513).

## REFERENCES

- (1). Venkatakrishnan AJ, Deupi X, Lebon G, Tate CG, Schertler GF, Babu MM. *Nature*. 2013; 494:185–194. [PubMed: 23407534]
- (2). Deupi X, Standfuss J. *Curr. Opin. Struct. Biol.* 2011; 21:541–551. [PubMed: 21723721]
- (3). Hubbell, WL.; Altenbach, C.; Hubbell, CM.; Khorana, HG. *Membrane Proteins*. Chemistry, DCRBT-A.; P., editors. Vol. Volume 63. Academic Press; 2003. p. 243-290.
- (4). Trzaskowski B, Latek D. *Curr. Med. Chem.* 2012; 19:1090–1109. [PubMed: 22300046]
- (5). Mahalingam M, Martínez-Mayorga K, Brown MF, Vogel R. *Proc. Natl. Acad. Sci. USA*. 2008; 105:17795–17800. [PubMed: 18997017]
- (6). Schoenlein RW, Peteanu LA, Mathies RA, Shank CV. *Science*. 1991; 254:412–415. [PubMed: 1925597]
- (7). Choe H, Kim Y, Park J, Morizumi T. *Nature*. 2011; 471:651–655. [PubMed: 21389988]
- (8). Struts AV, Salgado GFJ, Tanaka K, Krane S, Nakanishi K, Brown MF. *Journal of Molecular Biology*. 2007; 372:50–66. [PubMed: 17640664]
- (9). Altenbach C, Kusnetzow A. *Proc. Natl. Acad. Sci. USA*. 2008; 105:7439–7444. [PubMed: 18490656]

- (10). Farrens DL, Altenbach C, Yang K, Hubbell WL, Khorana HG. *Science*. 1996; 274:768–770. [PubMed: 8864113]
- (11). Arnis S, Hofmann KP. *Proc. Natl. Acad. Sci. USA*. 1993; 90:7849–7853. [PubMed: 8356093]
- (12). Knierim B, Hofmann KP, Ernst OP, Hubbell WL. *Proc. Natl. Acad. Sci. USA*. 2007; 104:20290–20295. [PubMed: 18077356]
- (13). Mahalingam M, Martinez-Mayorga K, Brown MF, Vogel R. *Proc. Natl. Acad. Sci. USA*. 2008; 105:17795–17800. [PubMed: 18997017]
- (14). Zaitseva E, Brown MF, Vogel R. *J. Am. Chem. Soc.* 2010; 132:4815–4821. [PubMed: 20230054]
- (15). Grossfield A. *Biochim. Biophys. Acta: Biomembr.* 2011; 1808:1868–1878.
- (16). Hornak V, Ahuja S, Eilers M. *J. Mol. Biol.* 2010; 396:510–527. [PubMed: 20004206]
- (17). Tikhonova I, Best R. *J. Am. Chem. Soc.* 2008; 130:10141–10149. [PubMed: 18620390]
- (18). Chen J, Im W, Brooks CL III. *J. Am. Chem. Soc.* 2006; 128:3728–3736. [PubMed: 16536547]
- (19). Im W, Feig M, Brooks CL III. *Biophys. J.* 2003; 85:2900–2918. [PubMed: 14581194]
- (20). Khavrutskii IV, Arora K, Brooks CL III. *J. Chem. Phys.* 2006; 125:174107–174108. III. [PubMed: 17100429]
- (21). Khandogin J, Brooks CL III. *Constant pH Molecular Dynamics with Proton Tautomerism. Biophysical journal.* 2005; 89:141–157. [PubMed: 15863480]
- (22). Sugita Y, Okamoto Y. *Chem. Phys. Lett.* 1999; 314:141–151.
- (23). Mackerell AD, Feig M, Brooks CL III. *J. Comput. Chem.* 2004; 25:1400–1415. [PubMed: 15185334]
- (24). MacKerell AD, Bashford D, Bellott, Dunbrack RL, Evanseck JD, Field MJ, Fischer S, Gao J, Guo H, Ha S, Joseph-McCarthy D, Kuchnir L, Kuczera K, Lau FTK, Mattos C, Michnick S, Ngo T, Nguyen DT, Prodhom B, Reiher WE, Roux B, Schlenkrich M, Smith JC, Stote R, Straub J, Watanabe M, Wiórkiewicz-Kuczera J, Yin D, Karplus M. *J. Phys. Chem. B.* 1998; 102:3586–3616.
- (25). Standfuss J, Edwards PC, D'Antona A, Fransen M, Xie G, Oprian DD, Schertler GFX. *Nature*. 2011; 471:656–660. [PubMed: 21389983]
- (26). Yan ECY, Kazmi MA, Ganim Z, Hou J-M, Pan D, Chang BSW, Sakmar TP, Mathies RA. *Proc. Natl. Acad. Sci. USA*. 2003; 100:9262–9267. [PubMed: 12835420]
- (27). Fahmy K, Sakmar TP, Siebert F. *Biochemistry*. 2000; 39:10607–10612. [PubMed: 10956053]
- (28). Periole X, Ceruso M, Mehler E. *Biochemistry*. 2004; 43:6858–6864. [PubMed: 15170322]
- (29). Khandogin J, Brooks CL III. *Biochemistry*. 2006; 45:9363–9373. [PubMed: 16878971]
- (30). Khandogin J, Chen J, Brooks CL III. *Proc. Natl. Acad. Sci. USA*. 2006; 103:18546–18550. [PubMed: 17116871]
- (31). Zhang BW, Brunetti L, Brooks CL III. *J. Am. Chem. Soc.* 2011; 133:19393–19398. [PubMed: 22026371]
- (32). Law SM, Zhang Bin W, Brooks CL III. *Protein Sci.* 2013:595–604. [PubMed: 23450521]

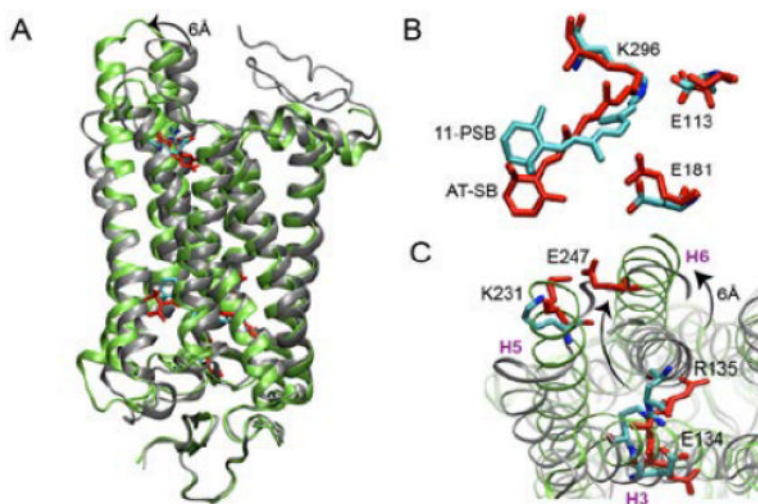


**Figure 1.**

A: Dark (grey; cyan) and Meta II (green; red) states of Rh. B, C: Regions involved in the two protonation-dependent switches.



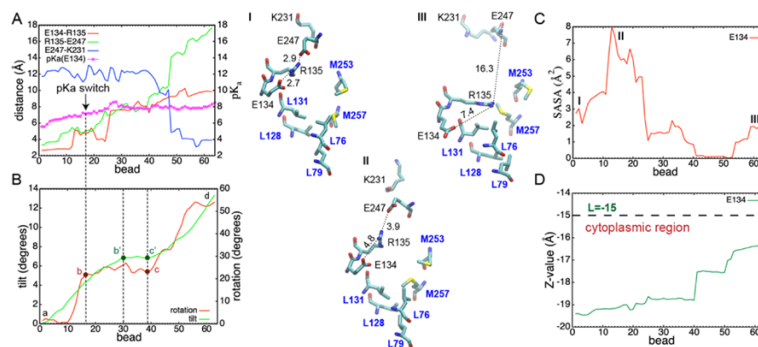


**Figure 2.**

Values computed along the Meta II<sub>a</sub> to Meta II pathway: pK<sub>a</sub> of E134 and average salt bridge distances measured between the closest oxygens and nitrogens of the corresponding acidic (E134, E247) and basic (R135, K231) residues, respectively (A); H6 tilt and rotation angles (B); SASA of the E134 side chain (C); and Z-value showing position of the E134 center of mass relative to the center of the lipid bilayer (D). Changes in the E(D)RY motif with respect to a hydrophobic barrier at different points of the pathway are shown for the end states (I and II) and in the region of the pK<sub>a</sub> switch (III).